Changes in the Electronic Properties of Si Nanocrystals as a Function of Particle Size

T. van Buuren, L. N. Dinh, L. L. Chase, W. J. Siekhaus, and L. J. Terminello
Chemistry and Materials Science Department, Lawrence Livermore National Laboratory, Livermore, California 94550
(Received 31 October 1997)

X-ray absorption and photoemission spectra have been used to measure the band edges of silicon nanocrystals with average diameters ranging from 1 to 5 nm. We compare the experimentally measured band edges to recent electronic structure calculations and find that the experimentally measured band gap is smaller than that predicted by theory. [S0031-9007(98)05892-X]

PACS numbers: 71.24.+q, 73.20.Dx, 79.60.Jv

The discovery of visible photoluminescence (PL) in porous Si and ultrafine Si has led to tremendous interest in their electronic and optical properties [1–3]. It is generally agreed that quantum confinement caused by the restricted size of the nanometer scale silicon particles is essential for the light-emitting properties [3–6]. A prediction of the quantum confinement model is that the energies of the valence band (VB) and conduction band (CB) edges are shifted relative to the bands of bulk silicon, leading to an increased energy gap. To date the change in the VB and CB edges as a function of the nanocrystal Si (nc-Si) size has not been experimentally determined. In this paper, we show how nc-Si with a narrow size dispersion as determined by scanned tip microscopies can be synthesized in a well-controlled environment. The electronic structure of the nc-Si is then investigated *in situ* using x-ray absorption and photoemission spectroscopies at beam lines 8.2 of the Stanford Synchrotron Radiation Facility and 8.0 of the Advanced Light Source.

Silicon nanocrystals were synthesized by thermal vaporization of Si in an argon buffer gas followed by exposure to atomic hydrogen to passivate the surface. Synthesis techniques have been reported earlier [3,6]. The substrate used to collect the nc-Si was a (111) oriented Ge wafer with a native oxide layer, mounted two inches directly above the evaporation boat. The size of the nc-Si was varied by increasing (or decreasing) the Si source temperature or the pressure of the Ar buffer gas. After synthesis, samples were transferred without air exposure into the ultrahigh vacuum analysis chamber. The measurements were made so that it was possible to measure both electron yield and photoemission without moving the sample, thus removing any possible effects of inhomogeneity on the sample. The resolution is 0.05 eV for the absorption spectra and 0.25 eV in the photoemission at a photon energy of 100 eV. X-ray absorption spectra were measured by total electron yield.

To measure the size of the nc-Si a highly oriented pyrolitic graphite (HOPG) substrate was used as a witness sample for each deposition on Ge. The basal plane of graphite was chosen as a substrate because all the carbon bonds in this plane are satisfied; also the surface is atomically flat, making it ideal for subsequent atomic force microscope (AFM) measurements of cluster size. Characterization of the size and morphology of the synthesized material was done *ex situ* using AFM. In Fig. 1(a) we show an AFM image on nc-Si deposited on HOPG by evaporation of Si at 1700 °C in an argon buffer gas of 112 mTorr. We find the silicon nanocrystals are mobile on the HOPG and gather at the step edges on the graphite surface or assemble into snowflakelike superclusters [7]. High resolution AFM shows that each of these structures is made up of individual nanocrystals in contact with the surface as shown in Fig. 1(a). An accurate lateral size is impossible to determine due to tip convolution; therefore, we use the height mode to determine the size of the nanocrystals. X-ray diffraction and high resolution transmission electron microscopy on these samples verify that the nc-Si are indeed crystalline and approximately spherical in shape [3]. In Fig. 1(b) we show the distribution in the diameter of the nc-Si determined from the z scale of the AFM image, which is calibrated with a set of known standards. The average diameter of the nanocrystals shown in Fig. 1 is 2.4 nm, with distribution in size that is approximately 25% of the average size. These results agree with *in situ* STM measurements reported earlier [3]. The size distribution is similar to the log-normal distribution found in ultrafine metal particles formed by evaporation in a reduced atmosphere of an inert gas [8].

The Si $L_{2,3}$-edge absorption is shown in Fig. 2(a) for a (111) silicon wafer and a nc-Si sample deposited on a Ge substrate by evaporation of Si at 1700 °C in a 40 mTorr Ar buffer gas. AFM measurements after spectroscopic characterization show that the average diameter of the clusters is approximately 1.6 nm. The bulk silicon reference sample was resistively heated to remove the surface oxide layer and then passivated with atomic hydrogen to remove the clean surface states [9]. The $L_{2,3}$ edge of the nanocrystalline samples is shifted to higher energy relative to the bulk silicon by 0.25 eV for the 1.6 nm clusters, as expected for quantum confinement, which raises the energy of the bottom of the conduction band as the nanocluster particle size is decreased. The energy of the L edge is obtained by extrapolating the linear part of the absorption edge just above the threshold to its intersection

0031-9007/98/80(17)/3803(4)$15.00 © 1998 The American Physical Society

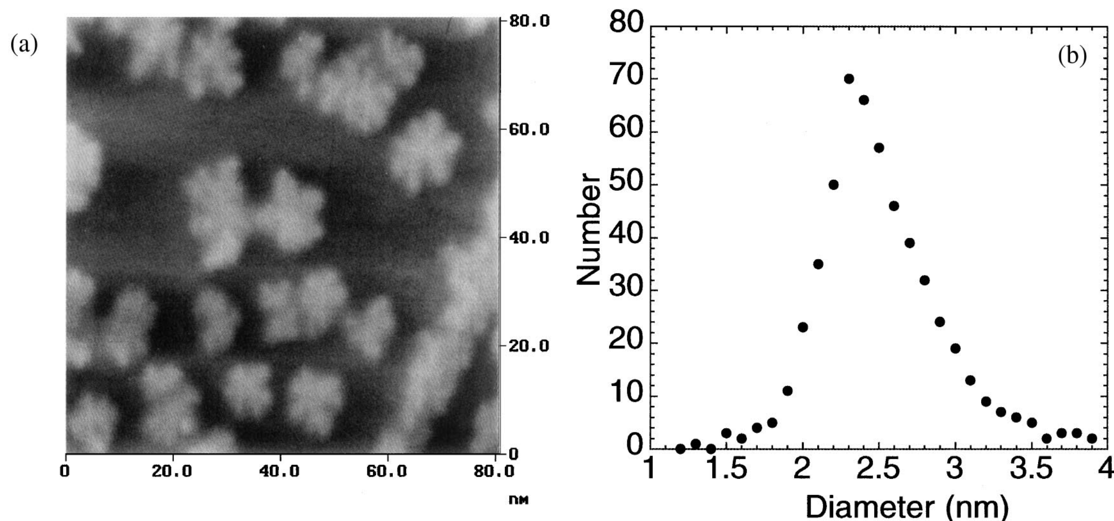

FIG. 1. (a) AFM image of silicon nanocrystals on the basal plane of HOPG formed by evaporation of Si at 1700 °C in an argon buffer gas of 112 mTorr. Note how the nanoclusters gather at the step edges on the graphite surface or assemble into snowflakelike superclusters. (b) The size distribution of the silicon nanocrystals determined from the AFM height mode.

with the baseline formed by the linear extrapolation of the pre-edge part of the spectrum. The shift of the band edge is defined as the difference between this extrapolation for the silicon nanocrystals and that for the bulk silicon. The well defined double threshold behavior associated with the 0.6 eV splitting of the Si $2p$ core level is less pronounced in the L edge of the nanocrystals, and the onset of the absorption edge in the nanocrystals is not as sharp as that in the bulk silicon. We attribute these features to a distribution of quantum shifts caused by the variation of particle size within the sample [10].

A photoemission spectrum for the VB of the nc-Si and bulk Si taken at a photon energy of 140 eV is shown in Fig. 2(b). The valence band edge of the nc-Si sample compared to the spectra for bulk silicon is shifted down by 0.50 eV with respect to the vacuum level, that is, an increase of 0.50 eV in the binding energy. For all nanocluster samples the valence band photoemission spectra were referenced to the Si $2p$ core level photoemission spectrum measured at the same photon energy and flux. Thus, the binding energy shift of the VB is due to electronic structure changes due to quantum confinement. We measured the top of the valence band relative to the low binding energy side of the Si core level. Subtracting these two values produces a valence band energy relative to the $2p$ core level which is independent of charging and the Fermi level position. We define the quantum shift in the valence band as the difference between the valence band edge measured relative to the $2p$ core level for the Si nanoclusters and the corresponding quantity for bulk silicon. It should be noted that the effects due to charging, if any, were minimal in all nanocluster photoemission spectra [11]. The peak in the nc-Si photoemission spectrum at 7 eV binding energy could be due to Si-H bonding feature or to the oxygen $2p$ orbital [12,13]. A small chemically shifted component we believe due to SiO_x is also observed in the $2p$ core level. Yet we do not see any silicon oxide features at 106 and 108 eV in the more bulk sensitive L-edge absorption spectrum [14]. This suggests that the oxide is on the surface of the clusters and the hydrogen passivation of the surface is not complete during the cluster synthesis. The valence band photoemission is particularly sensitive to even a fraction of a monolayer of surface oxygen because the oxygen $2p$ orbital has a significantly higher cross section at 140 eV photon energy than the Si $3s$ and $3p$ orbitals which make up the valence band [15]. We estimate the surface oxide coverage to be approximately $\frac{1}{2}$ of a monolayer and not a factor in the measurement of the VB maximum. We note that recent bulk sensitive and element specific soft x-ray fluorescence measurements of the valence band of silicon nanoclusters also show a shift in the VB maximum that is comparable to the photoemission results [6]. This confirms that the photoemission measurement is measuring the true silicon valence band shift, not just a surface state or surface species.

If the observed VB or CB shifts are due to quantum confinement, one would expect the size of the band shifts to increase as the particle size of the nanocrystalline Si is decreased. This observed effect is shown in Figs. 3(a) and 3(b) where we plot the shift in the conduction band edge and the shift in the valence band edge for Si nanocluster samples with different average sizes. The error bars in the energy axis of Figs. 3(a) and 3(b) indicate the measurement accuracy in determining the CB minimum, VB maximum. The horizontal error bars represent the full width at half maximum of the size distribution of the silicon nanoclusters. The x-ray absorption spectra has been modeled for several samples using a carefully measured size distribution and the best fit to the data in Fig. 3(a). We find that the absorption

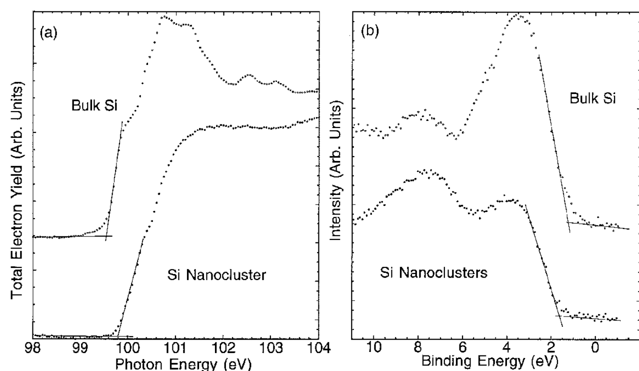

FIG. 2. (a) $L_{2,3}$ absorption spectra for bulk Si and nc-Si deposited on oxidized Ge with an average diameter of 1.6 nm. (b) Photoemission spectra for the valence band of bulk Si and the nc-Si with average diameter of 1.6 nm. The VB spectra were referenced to the Si $2p$ core level.

edge of the model spectra falls within the error bars of the experimental data [16]. The solid squares in both plots are theoretically predicted CB and VB shifts from a pseudopotential calculation of the electronic structure of spherical silicon quantum dots terminated with hydrogen [17]. The calculated size dependence of the CB minimum and VB maximum was found not to depend on the geometric shape of the quantum dot; similar VB and CB shifts are calculated for square and rectangular quantum dots. We note that the trend with cluster size of the experimental data looks very similar to the theory, but it is shifted down on the diameter scale by approximately 1 nm in the CB and 0.5 nm in the valence band. The calculated value for the conduction band shift includes a Coulomb correction term to account for the electron-hole Coulomb binding energy in the quantum dot. Yet it should be noted that the correction term assumes the hole to be in the valence band rather than the $2p$ core level which is the final state of the x-ray absorption process.

In the inset of Fig. 4 we plot the CB shift as a function of the valence band shift and show that the energy shift in the CB is correlated to the energy shift in the VB edge. All data points lie on a solid line with slope equal to two within experimental error. This ratio is in good agreement with earlier measurement of the ratio of VB shift to CB shift for porous silicon [11]. Various electronic structure calculations also predict a ratio of two for the valence to conduction band edge shifts in silicon quantum dots [17,18]. The band gap of the silicon nanoclusters can be determined by adding the measured conduction band shift to the measured valence band shift and the band gap of bulk silicon. For samples for which only the CB shift is known from core level absorption, an estimate of the band gap is obtained from

$$E_{\mathrm{gap}} = 3\Delta\mathrm{CB} + 1.1\ \mathrm{eV},$$

since the VB shift is equal to twice the CB band shift. In Fig. 4 we plot the band gap of the nanoclusters as a function of the measured diameter, and compare this

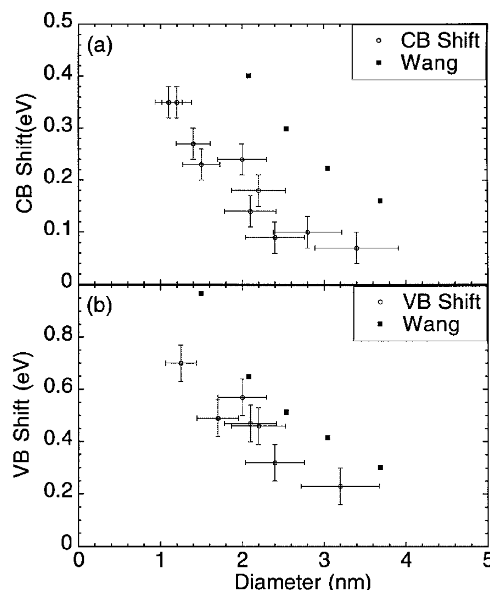

FIG. 3 (a) The conduction band (CB) edge shift and (b) the valence band (VB) edge shift as a function of nanocrystal diameter. The solid squares represent the theoretically predicted VB and CB edge shifts for a hydrogen terminated spherical silicon quantum dot.

data with recent PL and extended x-ray absorption data from oxygen terminated silicon nanoclusters [19] and with theoretical results for spherical silicon clusters terminated with hydrogen [17]. We find that the photoemission band gap agrees with the data from Schuppler *et al.* for particle sizes smaller than 40 A [19]. Those authors

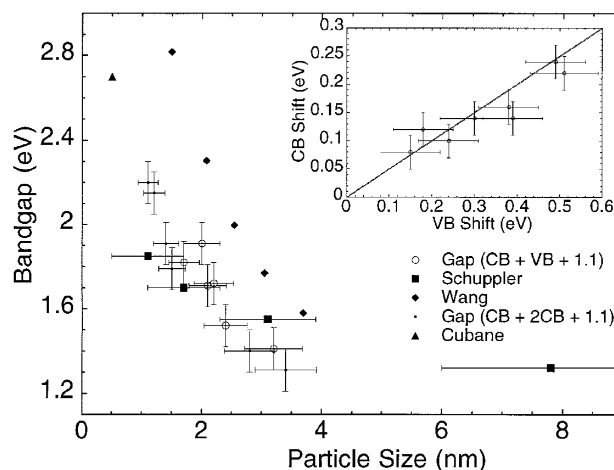

FIG. 4. Band gap of the nc-Si as a function of particle size. Photoelectron data are given by the open circles (ΔCB + ΔVB + 1.1 eV) and filled circles (3ΔCB + 1.1 eV); the PL data of Schuppler *et al.* [18] for oxidized silicon nanoclusters is given with the filled squares; the pseudopotential calculation of Wang [16] is given with the filled diamonds and the cubane data [21] are given by the filled triangle. Inset: The CB shift versus the VB shift for a series of nanoclusters. The solid line represents a 2:1 ratio between the VB shift and the CB shift.

point out that correlations between average size and PL are unreliable for particles of ~80 A or greater because their size distribution is too broad. Also there is some question as to whether the PL from nc-Si terminated in oxide is a direct band to band transition or if the surface oxide is somehow responsible [20]. The general trend of the experimentally determined band gap as a function of size agrees with the theory but in all cases the calculated band gap is larger than the measured band gap. This may, in part, be due to the fact that the clusters in the calculation are perfect spheres terminated with hydrogen, whereas the measured clusters have an unknown surface reconstruction that has at least a partial monolayer of oxide on the surface. It is possible that there is a substrate-cluster interaction and the contact surface of the cluster is flattened due to these contact forces. This would cause the cluster height measured by the AFM to be smaller than the actual diameter of the nanoclusters. This effect has been observed in recent TEM and AFM measurements of gold clusters deposited on the surface of HOPG [21]. It was found that the AFM measured diameter of the gold cluster was 10% smaller than that of the TEM result. This effect is not large enough to explain the difference between experiment and theory. A further source of uncertainty is the effect of contact between the clusters deposited on the substrate. It is interesting to note that recent soft x-ray emission measurements on a cubic Si_8 cluster, octasilacubane, has reported the band gap to be approximately 2.7 eV [22]. This agrees favorably with an extrapolation of the trend of the experimental data to a size of 0.5 nm, the approximate size of Si_8.

In conclusion, we were able to synthesize silicon nanocrystals with a fairly selective size as measured with an AFM. We observed shifts in both the CB and the VB edges, indicating quantum size effects in the band structure of the nanocrystals, and, for the first time, we were able to correlate these shifts with a known size of nanocrystals. We find the general trend of the band gap versus size curve agrees well with theory, but in all cases the experimental band gap is smaller than what is predicted by theory.

This work was supported by the Division of Materials Sciences, Office of Basic Energy Science, U.S. Department of Energy, and performed under the auspices of the U.S. Department of Energy by Lawrence Livermore National Laboratory under Contract No. W-7405-ENG-48. This work was done at SSRL and the ALS which are supported by DOE Contracts No. DE-AC03-76SF00515 and No. DE-AC03-76SF00098, respectively.

[1] T. Canham, Appl. Phys. Lett. **57**, 1046 (1990).
[2] H. Takagi, H. Ogawa, Y. Yamazaki, A. Ishizaki, and T. Nakagiri, Appl. Phys. Lett. **56**, 379 (1990).
[3] L. N. Dinh, L. L. Chase, M. Balooch, W. J. Siekhaus, and F. Wooten, Phys. Rev. B **54**, 5029 (1996).
[4] F. Koch, V. Petrova-Koch, and T. Muschik, J. Lumin. **57**, 271 (1993).
[5] P. D. J. Calcott, K. J. Nash, L. T. Canham, M. J. Kane, and D. Brumhead, J. Lumin. **57**, 257 (1993).
[6] T. van Buuren, L. N. Dinh, I. Jimenez, L. J. Terminello, M. Grush, T. A. Calcott, and J. A. Carlisle, Mater. Res. Soc. Symp. Proc. **452**, 171 (1996).
[7] L. Bardotti, P. Jensen, A. Hoareau, M. Treilleux, and B. Cabaud, Phys. Rev. Lett. **74**, 4694 (1995).
[8] C. G. Granqvist and R. A. Buhrman, J. Appl. Phys. **47**, 2200 (1976).
[9] F. J. Himpsel, G. Hollinger, and R. A. Pollack, Phys. Rev. B **28**, 7014 (1983).
[10] T. van Buuren, T. Tiedje, Y. Gao, J. R. Dahn, and B. M. Way, Appl. Phys. Lett. **60**, 3013 (1992).
[11] T. van Buuren, T. Tiedje, J. R. Dahn, and B. M. Way, Appl. Phys. Lett. **63**, 2911 (1993).
[12] G. Hollinger and F. J. Himpsel, J. Vac. Sci. Technol. A **1**, 640 (1983).
[13] S. Ciraci, R. Butz, E. M. Oellig, and H. Wagner, Phys. Rev. B **30**, 711 (1984).
[14] M. Kasrai, W. N. Lennard, R. W. Brunner, G. M. Bancroft, J. A. Bardwell, and K. H. Tan, Appl. Surf. Sci. **99**, 303 (1996).
[15] J. J. Yeh and I. Lindau, At. Data Nucl. Data Tables **32**, 1 (1985).
[16] T. van Buuren and L. L. Chase (to be published).
[17] Lin-Wang Wang and A. Zunger, *Nanocrystalline Semiconductor Materials,* edited by P. V. Kamat and D. Meisel (Elsevier Science, New York, 1996).
[18] S. Y. Ren and J. D. Dow, Phys. Rev. B **45**, 6492 (1992).
[19] S. Schuppler, S. L. Friedman, M. A. Marcus, D. L. Adler, Y. H. Xie, F. M. Ross, Y. J. Chabal, T. D. Harris, L. E. Brus, W. L. Brown, E. E. Chaban, P. F. Szajowski, S. B. Christman, and P. H. Citrin, Phys. Rev. B **52**, 4910 (1995).
[20] Y. Kanemitsu, T. Ogawa, K. Shiraishi, and K. Takeda, Phys. Rev. B **48**, 4883 (1993).
[21] W. Mahoney, D. M. Schaefer, A. Patil, R. P. Andres, and R. Reifenberger, Surf. Sci. **316**, 383 (1994).
[22] Y. Muramatsu, M. Sugiyama, S. Maeyama, K. Furukawa, K. Ebata, M. Fujino, S. Kawai, and M. Motoyama (to be published).